ISBN: 978-3-95450-231-8 ISSN: 2673-5490 doi: 10.18429/JACoW-IPAC2023-TUPL139

C-BAND PHOTOINJECTOR RADIOFREQUENCY CAVITY DESIGN FOR ENHANCED BEAM GENERATION*

H. Xu†, P. M. Anisimov, W. C. Barkley, G. R. Bustos, E. I. Simakov
Los Alamos National Laboratory, Los Alamos, NM, USA

Abstract

We present our 1.6-cell 5.712-GHz radiofrequency cavity design for a photoinjector under development for producing intense electron bunches with 250-pC beam charge and normalized emittance below 100 nm rad for cryogenic temperature operation. The cavity cell profile was designed by SLAC and UCLA, optimized for maximal shunt impedance and minimal peak magnitude of the electric and magnetic field. The π-mode accelerating fields are established in the cells with power coupled into each cell individually through the slot on the sidewall, and the peak electric field magnitude is tuned to be equal in the two cells. The coupling waveguide network was designed to achieve critical coupling at the port of the input power waveguide and to achieve the desired power distribution. The completed cavity design is intended for initial high-gradient test at room temperature.

INTRODUCTION

High-brightness electron beams are desired in particle accelerator applications for light sources, e. g., X-ray free electron lasers, and for future electron-positron colliders [1]. In order to obtain an electron beam with higher brightness, greater beam current and smaller emittance are needed. One solution to meet this demand is using a radiofrequency (RF) photoinjector that operates at cryogenic temperatures and under intense accelerating fields, to provide bunched electron beams with both enhanced beam current and minimized emittance. Cryo-temperature metallic RF accelerator cavities demonstrated accelerating gradients up to 250 MV/m at X-band, which was significantly higher than the gradient limit observed at room temperature (~100 MV/m). This technology can be readily applied to building high-gradient RF photoinjectors. The intense electric field in the cryo-temperature photoinjector in our study brings about two benefits. First, the high accelerating gradient allows fast acceleration of the electron beam, so that the beam emittance dilution due to the space charge force is mitigated; second, the enhanced electric field on the photocathode tends to extract electron emission with an increased current.

At Los Alamos National Laboratory (LANL), we are performing research and development on a 5.712-GHz RF photoinjector to operate at 77 K, with the photocathode witnessing an electric field above 100 MV/m and providing electron beam bunch charge up to 250 pC over 5-6 ps. The first photoinjector cavity test will be carried out at room temperature at LANL [2], for the purpose of examining the performance of the RF design of the cavity, without involving the cathode plug. This cavity is currently under fabrication. In this work, all RF analysis was performed using the CST Frequency Domain Solver, and all mechanical design was performed in SOLIDWORKS.

DESIGN OVERVIEW

The 5.712-GHz photoinjector RF cavity uses a 1.6-cell design. The model of the RF cavity is shown in Fig. 1. The cavity was designed to be made of oxygen-free high thermal conductivity (OFHC) copper. We designate the cell accommodating the photocathode as the "cathode cell," and the cell with the full length, "full cell." The profile of the individual cells and the power coupling design of the cells from the side were provided by SLAC and UCLA [3], optimized for mitigated peak electric and magnetic fields, and for maximized shunt impedance. The photoinjector cavity was designed to operate at the π-mode, i. e., the RF phase difference between the two cells was 180 deg. Each individual cell of the cavity operates at the TM_{01}-mode. Because the initial high power test of the cavity will not involve electron beam generation, the cavity was designed with the critical coupling of the RF power, measured at the input waveguide port. The input power is fed to the cavity through the standard WR187 waveguide.

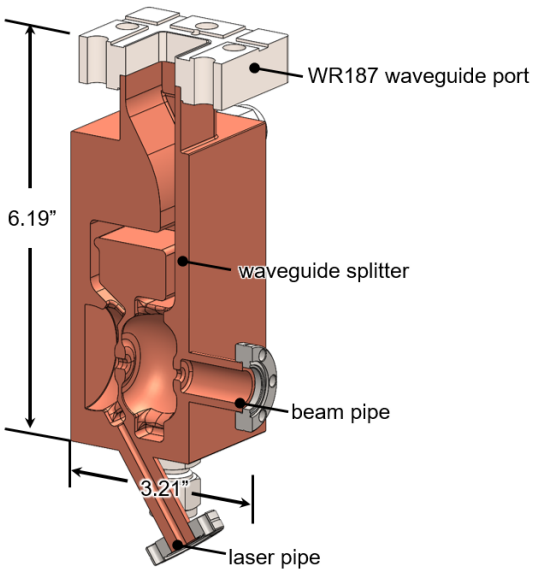

Figure 1: Longitudinal cross section view of the photoinjector RF cavity mechanical design.

The input RF power enters the cavity through the WR187 waveguide port, and flows through the waveguide taper to

* Work supported by the Laboratory Directed Research and Development program of Los Alamos National Laboratory under project number 20230011DR.
† haoranxu@lanl.gov

ISBN: 978-3-95450-231-8 ISSN: 2673-5490 doi: 10.18429/JACoW-IPAC2023-TUPL139

arrive at the waveguide splitter. The waveguide splitter divides the power for the cathode cell and for the full cell, respectively, so that the peak electric field magnitude in the individual cells will be identical. The central axis of the laser pipe points at the center of the cathode plane. The beam pipe inner diameter was designed to be much larger than the beam aperture diameter of the cells, for the purpose of accommodating the electron beam transverse size variation during the transport.

INDIVIDUAL CELL TUNING

The first task of the RF cavity design was to ensure that both the cathode cell and the full cell achieved critical coupling at the resonant frequency of 5.712 GHz. Figure 2 shows the vacuum volume model of the cathode cell and the full cell, along with the coupling slots on the side, connecting to the waveguide splitter.

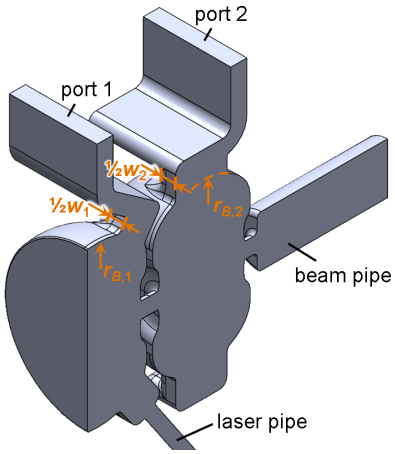

Figure 2: Vacuum volume model of the cathode cell and the full cell, with the tuning parameters labeled.

The sidewall profile of the individual cells takes an elliptical shape. The resonant frequency was tuned by varying the minor radius of the elliptical curve, in each cell ($r_{B,1}$ and $r_{B,2}$). The width, i. e., the transverse size, of the coupling slot in each cell (w_1 and w_2) was varied to adjust the reflection coefficient magnitude seen at the port 1 and 2, as indicated in Fig. 2.

The finalized reflection coefficient magnitude was observed below −30 dB, at the resonant frequency of 5.712 GHz, for each cell. The unloaded quality factor was calculated to be 14695 for the cathode cell, and 13603 for the full cell. The time-dependent shunt impedance of the full cell, when the electron beam being accelerated travels at the speed of light, is 3.09 MΩ, or 118 MΩ/m.

WAVEGUIDE SPLITTER

The second task was to build the model of the waveguide splitter, as shown in Fig. 3. The port 1 feeds the RF power to the cathode cell, and port 2, the full cell. The input RF power comes in through the port 3. The function of the waveguide splitter is to divide the input RF power for the individual cells, so that the maximal electric field magnitude in the cells will be identical. Meanwhile, the reflection coefficient at port 3 needs to be minimized.

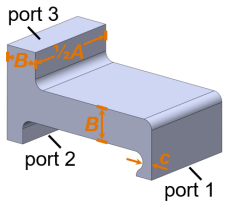

Figure 3: Vacuum volume model of the waveguide splitter, with the tuning parameters labeled.

The waveguide splitter dimension A adjusts the RF phase advance between the port 1 and 2. Increasing A causes the phase difference to become greater. The reflection coefficient magnitude was minimized by adjusting both dimension A and B of the waveguide splitter. The RF power division into the port 1 and 2 is determined by the choke size c. Decreasing the choke size c reduces the RF power coupled through the port 2, into the cathode cell. The finalized design achieved $|S_{33}| < -60$ dB at 5.712 GHz.

HORN TAPER OPTIMIZATION

The third task was to come up with a waveguide taper design to match the waveguide splitter to the port of the standard WR187 waveguide. The vacuum volume model of the waveguide taper is provided in Fig. 4. The port 3 connects to the waveguide splitter, and the port 4 connects to the standard WR187 waveguide. The input RF power is fed through port 4 to the RF cavity.

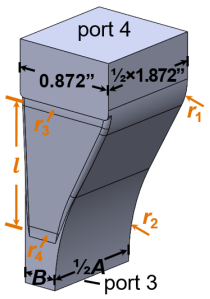

Figure 4: Vacuum volume model of the waveguide taper connecting the waveguide splitter to the WR187 waveguide port. The tuning dimensions are labeled in orange, while the fixed dimensions were shown in black.

As Fig. 4 illustrates, the waveguide splitter dimensions A and B have been determined beforehand. The four fillet radii and the length of the taper section serve as the variables, to be used in the CST Frequency Domain Solver optimizer for minimized input power reflection at port 4. The finalized design achieved $|S_{44}| < -60$ dB at 5.712 GHz. In addition, the design of the fillets on the edges along the taper section were applied to meet the requirements of fabrication.

ISBN: 978-3-95450-231-8 ISSN: 2673-5490 doi: 10.18429/JACoW-IPAC2023-TUPL139

CAVITY RF ANALYSIS

The final task of the cavity design was the global fine tuning of the design parameters, after putting together the individually designed cavity cells, waveguide splitter, and the horn taper. The finalized cavity design exhibited 180-deg RF phase difference between the cathode cell and the full cell. The peak electric field in the individual cells was tuned to be identical. The entire cavity showed a resonant frequency at 5.712 GHz, with an unloaded quality factor of 14170. The distribution of the RF fields is shown in Fig. 5.

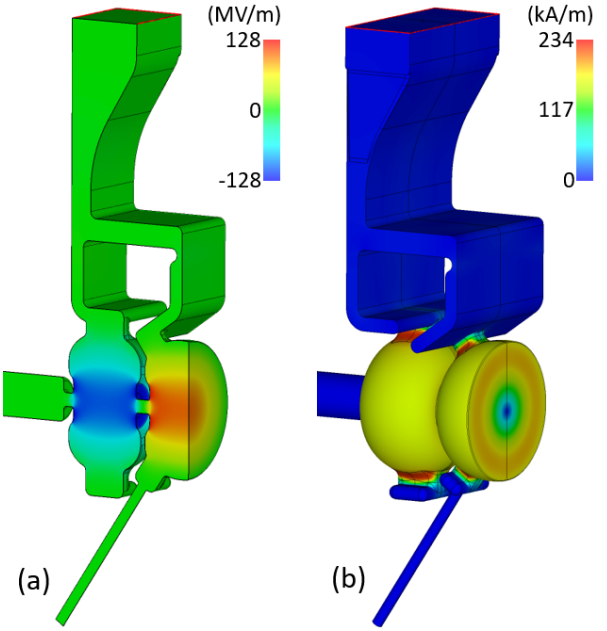

Figure 5: RF field distribution inside the photoinjector cavity, with 100-MV/m electric field at the cathode plane center. (a) Longitudinal electric field. (b) Magnetic field magnitude.

The distribution of the longitudinal electric field is provided in Fig. 5a, where the highest electric field, at the cathode plane center, is 100 MV/m. The peak electric field is 128 MV/m, located on the structure inner surface, close to the beam aperture. Fig.ure 5b shows the distribution of the magnetic field magnitude. The peak magnetic field is 234 kA/m, located at the coupling slot to the cathode cell.

On the beam axis, the distribution of the RF electric field magnitude is plotted in Fig. 6. It can be seen that the maximal electric field on the beam axis is E_m = 106 MV/m, located in the full cell. The accelerating gradient of the full cell, when the electrons being accelerated travels at the speed of light, is 63.2 MV/m. In the full cell, the ratio of the peak surface electric field to the gradient was calculated to be 2.0.

In our planned high power test of the RF photoinjector cavity, 1.4 MW of the RF power will be needed to have 100 MV/m maximal electric field on the cathode plane; we also have the plan for achieving a significantly higher maximal electric field on the cathode plane, at 240 MV/m, which will require an input RF power of 8.0 MW.

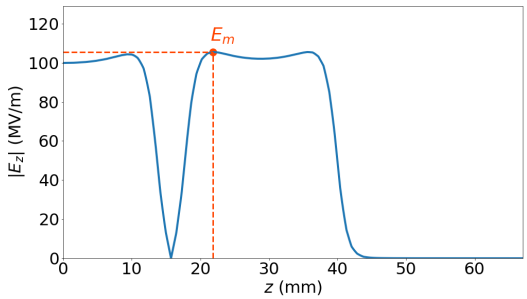

Figure 6: Distribution of the RF electric field magnitude on the beam axis.

FABRICATION AND CHALLENGES

The copper cavity body was designed to be machined in halves, and then brazed together. The stainless steel flanges would be brazed on the ports of the cavity. One pair of tuners are used for the cathode cell and the full cell, respectively, on the opposite sides, in the horizontal direction.

The profile of the cells in the cavity presents significant complexity. Fabrication tolerance is desired at 0.001 inch. In Fig. 2, 0.001-inch increase of $r_{B,1}$ or $r_{B,2}$ will cause the resonant frequency of the respective cell to reduce by ~5 MHz. In Fig. 3, 0.001-inch increase of the choke size c will cause ~1% increase in the ratio of the peak electric field in the cathode cell to that in the full cell.

CONCLUSIONS

We performed simulations and the mechanical design of an RF cavity for building a 1.6-cell photoinjector. The design met the goals of achieving identical peak electric field in the cathode cell and in the full cell, and of presenting a 180-degree RF phase difference between the two cells.

The high power test of the cavity will be performed at room temperature, for examining the high-gradient performance of the RF design, and for providing guidance for developing an RF photoinjector cavity to operate under intense accelerating field at cryogenic temperatures.

REFERENCES

[1] R. R. Robles *et al.*, "Versatile, high brightness, cryogenic photoinjector electron source," *Phys. Rev. Accel. Beams*, vol. 24, no. 6, p. 063401, 2021. doi:10.1103/PhysRevAccelBeams.24.063401

[2] E. I. Simakov *et al.*, "Update on the status of C-Band research and facilities at LANL," in *Proc. NAPAC 2022*, Albuquerque, USA, Aug. 2022, paper THYD3, pp. 855-858. doi:10.18429/JACoW-NAPAC2022-THYD3

[3] G. E. Lawler *et al.*, "Design of a high-power RF breakdown test for a cryocooled C-band copper structure," in *Proc. NAPAC 2022*, Albuquerque, USA, Aug. 2022, paper TUPA81, pp. 516–518. doi:10.18429/JACoW-NAPAC2022-TUPA81